Structural and Dynamical Properties of Semirigid Polyelectrolyte Solutions: A Light-Scattering Study

Eric Buhler* and Marguerite Rinaudo

Centre de Recherche sur les Macromolécules Végétales (CNRS), Université Joseph Fourier de Grenoble, BP 53, 38041 Grenoble Cedex, France

Received August 5, 1999; Revised Manuscript Received December 3, 1999

ABSTRACT: Dynamic and static light-scattering experiments were performed on aqueous solutions of the highly charged semiflexible polyelectrolyte chitosan in the dilute and the semidilute regime. In the dilute regime, typical good solvent behavior is found. However, in the overlapped regime the time autocorrelation function of the scattered electric field is found to be bimodal. The short time relaxation has a typical q^2 dependence, characteristic of diffusion, and the long time relaxation an approximately q^2 dependence, where q is the scattering wave vector. Static and dynamic light-scattering experiments were carried out to analyze the two modes. The fast mode is attributed to the relaxation of concentration fluctuations characterized by a cooperative diffusion mechanism of the polymer network meshes. The slow relaxation time appears to be related to the diffusion of polymer associations. The effect of the excess of salt concentration and polymer concentration was investigated.

1. Introduction

In the present paper, dynamic and static light-scattering experiments were performed on aqueous solutions of the highly charged semiflexible polyelectrolyte chitosan. Chitin and chitosan are important polysaccharides extracted from different sources (crabs or shrimp shells, etc....). These polymers are composed of $\beta1{\rightarrow}4$ D-glucosamine units with a variable degree of N-acetylation. When the average degree of N-acetylation is lower than approximately 0.5, the polymers are called chitosans, and they become soluble in aqueous solutions in the presence of acids such as acetic acid.[1]

In solutions of polyelectrolytes, made from linear flexible polymers, an essential parameter is the polymer chain rigidity, which is strongly influenced by the ionic strength and in particular by the polyelectrolyte concentration. Electrostatic repulsion between charges along the chain will affect the local flexibility of the chain and will tend to increase the global size of the polyion. For polyelectrolytes the total persistence length, L_t, is written as[2]

$$L_t = L_0 + L_e \tag{1}$$

The total persistence length represents the effective rigidity of the polyelectrolyte as the sum of two contributions: the intrinsic persistence length L_0 due to the rigidity of the uncharged chain and the electrostatic persistence length L_e arising from the repulsion between ionic sites. The value of the intrinsic persistence length of the chitosan is estimated between 50 and 150 Å;[1] the rigidity of this polymer is quite important even in high ionic strength solutions. For polysaccharides the electrostatic contribution L_e is easily much smaller than the intrinsic contribution L_0. This is the reason chitosan and polysaccharides, in general, are called semirigid or rigid polymers. Several workers[2-5] have calculated the electrostatic contribution to the persistence length L_e. Odijk[2] and Skolnick and Fixman,[3] assuming a Debye−Hückel potential, if the condensation model applies,[6] have derived a formula giving L_e

$$L_e = \frac{1}{4\kappa^2 l_B} \qquad \text{for } \lambda_0 > 1 \tag{2}$$

where l_B is the Bjerrum length ($l_B = e^2/\epsilon_0 kT = 7.13$ Å in water, ϵ_0 is the dielectric permittivity of the solvent, and e is the elementary charge) and κ^{-1} is the Debye−Hückel screening length related to the concentration of the counterions. The structural charge parameter $\lambda_0 = 1.3$ in our case[1] ($\lambda_0 = e^2/\epsilon_0 kTa$, a being the distance between two ionic sites).

$$\kappa^2 = 8\pi l_B c \tag{3}$$

In eq 3, c is the concentration of the noncondensed 1:1 counterions. Equation 2 is valid if $\kappa L_t \gg 1$, which is true for polyelectrolytes near the rod limit or at least for polyelectrolytes having a high intrinsic stiffness. Since chitosan has a larger intrinsic persistence length L_0 than the electrostatic persistence length L_e (at least for external salt concentration larger than 3×10^{-3} M), this polymer is characterized by a high rigidity, even in the high ionic strength solutions (κ^{-1} small).

In the present paper, we report the results of the light-scattering experiments performed on 0.3 M acetic acid solutions of a 190 000 semiflexible polyelectrolyte chitosan for polymer concentrations ranging from 10^{-4} to 4×10^{-3} g/cm³, for excess of salt concentrations (sodium acetate) ranging from 0.05 to 0.2 M and at a temperature $T = 25$ °C. In the dilute regime, typical good solvent behavior is found. However, in the overlapped regime, the time autocorrelation function of the scattered electric field measured by dynamic light scattering is found to be bimodal. A double exponential correlation function is interpreted as consisting of two relaxations: a fast relaxation and a slow relaxation. Over the past two decades, these general effects have been reported for nearly all classes of charged macromolecular systems: charged biological polymers,[7-10] synthetic polyelectrolytes in aqueous, and no aqueous solutions.[11-23] There has been some debate about whether the slow mode of diffusion often reported for dynamic light-scattering experiments on polyelectrolyte solutions corresponds to the formation of domains,[20,21] aggregates,[22,23] or supramolecular structures[7-9,13-17] or gives evidence of a reptation mechanism.[11] The fast mode has been attributed to coupled diffusion of polyions and low-molecular-weight counterions[7,10,11] or thermally excited displacements of polymer segments between entangle-

ments.[13] To understand the origin of the fast and the slow mode, the scattering wave vector **q** dependencies for the scattering intensity and for the amplitudes and characteristic times associated with the relaxation modes must be carefully analyzed. This can be done by a combination of the static and the dynamic light-scattering techniques, which provides a powerful tool to better understand the physical mechanisms that are at the origin of dynamical behavior of this semirigid polyelectrolyte system. The slow mode is interpreted as reflecting the diffusion of polymer associations, whereas the fast mode relaxation results from the cooperative diffusion of the meshes of the polymer network.

In section 2 of the paper, we describe materials and experimental techniques used in this study. In section 3, we report the results of the experiments and discuss these results.

2. Materials and Methods

2.1. Sample Characteristics. We have investigated solutions of the 190 000 polysaccharide chitosan, which is a semirigid polyelectrolyte. The polysaccharide chitosan belongs to a family of linear cationic biopolymers obtained from alkaline N-deacetylation of chitin, which is the second most abundant polymer in nature. The studied chitosan is a 190 000 commercial polymer from PROTAN composed of β 1→4 D-glucosamine units with a degree of N-acetylation equal to 12%. The polydispersity was determined using GPC experiments and is equal to the ratio $M_w/M_n = 1.3$, where M_w is the weight-average molecular weight and M_n the number-average molecular weight.[1] The contour length is equal to 6000 Å. In acid conditions, chitosan is water-soluble due to the presence of protonated amino groups and it exhibits a polyelectrolyte character. The solutions were investigated in the polymer concentration range 1×10^{-4} to 4×10^{-3} g/cm^3 at the temperature $T = 25$ °C and in the solvent 0.3 M acetic acid (CH$_3$COOH) in the presence of sodium acetate (CH$_3$COONa). The concentration of sodium acetate (excess of salt) was varying between 0.05 and 0.2 M. For a 0.3 M concentration in acetic acid, all the amino groups are protonated and chitosan exhibits a high polyelectrolyte character.[1]

To carry out static and dynamic light-scattering experiments all the solutions were filtered directly into the light-scattering cells through 0.1 or 0.2 μm Sartorius cellulose nitrate membranes. No aging effects were observed with our solutions.

2.2. Viscosity Measurements. Viscosity measurements were made with a Low Shear 30 coaxial viscometer. This allowed measurements to be made on the Newtonian plateau. The viscosity measurements were made in the range of polymer concentration from 10^{-4} to 4×10^{-3} g/cm^3, which includes the domain over which the light-scattering experiments were performed.

2.3. Static Light Scattering. Static light-scattering (SLS) and dynamic light-scattering (DLS) experiments were performed by means of a spectrometer equipped with an argon ion laser (Spectra Physics model 2020) operating at $\lambda = 488$ nm, an ALV-5000 correlator from ALV, Langen-FRG Instruments, a computer-controlled and stepping-motor-driven variable-angle detection system and a temperature-controlled sample cell. The temperature was (25 ± 0.1)°C unless otherwise noted. The scattering spectrum was measured through a band-pass filter (488 nm) and a pinhole (200 μm for the static experiments and 100 or 50 μm for the dynamic experiments) with a photomultiplier tube (ALV).

In the SLS experiments one measures the excess of scattered intensity $I(q)$ with respect to the solvent, where the magnitude of the scattering wave vector **q** is given by

$$q = \frac{4\pi n}{\lambda}\sin\frac{\theta}{2} \tag{4}$$

In eq 4, n is the refractive index of the solvent (1.34 for the

water at 25 °C), λ is the wavelength of light in the vacuum, and θ is the scattering angle. In our experiments, the scattering angle θ has been varied between 20 and 150°, which corresponds to scattering wave vectors q in the range 6×10^{-4} to 3.2×10^{-3} Å^{-1}. Corrections to the absolute scattering intensities $I(q)$ (i.e., excess Rayleigh ratio) were made using a toluene sample reference for which the excess Rayleigh ratio is well-known.

One can use a virial expression for the osmotic pressure in dilute regime to deduce the following relation

$$\frac{Kc}{I(q,c)} = \frac{1}{M_w}\left[1 + q^2\frac{R_G^2}{3} + ...\right] + 2A_2 Q(q,c)c + ... \tag{5}$$

where, for example, the function $Q(q,c)$ is approximately unity for flexible polymer chains, but not for spheres,[24] $Q(0,c)$ is equal to 1 in any case. c is the polymer concentration and A_2 is the second virial coefficient, which describes the polymer–solvent interactions. The scattering constant is $K = 4\pi^2 n^2 (\mathrm{d}n/\mathrm{d}c)^2/N_A\lambda^4$ where $\mathrm{d}n/\mathrm{d}c$ is the refractive index increment and N_A is Avogadro's number. The $\mathrm{d}n/\mathrm{d}c$ of the polysaccharide chitosan in the solvent 0.3 M acetic acid + sodium acetate is equal to 0.195.[1] Plots of $c/I(q,c)$ vs q^2 were extrapolated to $q = 0$ to give intercepts $c/I(0,c)$. For infinite dilute solutions, the average radius of gyration R_G can be determined from the intercept and the initial slope of these plots using a scattering inverse Lorentzian law of the form[24]

$$\frac{c}{I(q,c)} = \frac{c}{I(0,0)}\left[1 + \frac{q^2 R_G^2}{3}\right] \quad \text{with } c \to 0 \tag{6}$$

The weight-average molecular weight[24] M_w can be obtained using

$$\frac{Kc}{I(0,c)} = \frac{1}{M_w} + 2A_2 c \tag{7}$$

2.4. Dynamic Light Scattering. In the dynamic light-scattering experiments (DLS), the normalized time autocorrelation function $g^{(2)}(q,t)$ of the scattered intensity is measured.[24]

$$g^{(2)}(q,t) = \frac{\langle I^*(q,0)I(q,t)\rangle}{\langle I(q,0)\rangle^2} \tag{8}$$

The latter can be expressed in terms of the field autocorrelation function or equivalently in terms of the autocorrelation function of the concentration fluctuations $g^{(1)}(q,t)$ (i.e., the time autocorrelation function of the scattered electric field) through

$$g^{(2)}(q,t) = A + \beta|g^{(1)}(q,t)|^2 \tag{9}$$

where A is the baseline and β the coherence factor which in our experiments is equal to 0.7–0.9. The normalized dynamical correlation function $g^{(1)}(q,t)$ of polymer concentration fluctuations is defined as

$$g^{(1)}(q,t) = \frac{\langle\delta c^*(q,0)\delta c(q,t)\rangle}{\langle\delta c(q,0)^2\rangle} \tag{10}$$

where $\delta c(q,t)$ and $\delta c(q,0)$ represent fluctuations of polymer concentration at time t and zero, respectively.

In our experiments, the inspection of the angular dependence shows that the relaxation in dilute regime is diffusive with characteristic time inversely proportioned to q^2. Our dilute solutions were characterized by a single relaxation mechanism. For these solutions we have adopted the classical cumulant analysis.[25] This analysis provides the variance of the correlation function and the first reduced cumulant $(\tau q^2)^{-1}$ where τ is the average relaxation time of $g^{(1)}(q,t)$. The extrapolation of $(\tau q^2)^{-1}$ to $q = 0$ yields the values of the mutual diffusion constant D. The latter is related to the average hydrodynamic radius R_H of the macromolecules through

$$D = \frac{kT}{6\pi\eta_s R_H} = \left(\frac{1}{\tau q^2}\right)_{q^2=0} \tag{11}$$

where k is the Boltzman constant, η_s the solvent viscosity, and T the absolute temperature.

Figure 1 shows log–log plots of $g^{(1)}(q,t)$ for solutions of chitosan at two different polymer concentrations in the solvent 0.3 M CH_3COOH + 0.05 M CH_3COONa and at $T = 25$ °C. The scattering angle θ is equal to 90°. The two polymer concentrations are 3×10^{-4} and 2×10^{-3} g/cm³. In the low concentration range, $g^{(1)}(q,t)$ is a single exponential, whereas at higher concentration, $g^{(1)}$, the autocorrelation function of scattered electric field can be described by a sum of two relaxations widely separated in time (see Figures 1 and 2).

$$g^{(1)}(q,t) = \frac{\langle E^*_{fast}(q,0)E_{fast}(q,t)\rangle + \langle E^*_{slow}(q,0)E_{slow}(q,t)\rangle}{\langle I(q)\rangle}$$

$$g^{(1)}(q,t) = A_{fast}(q)\exp\left(\frac{-t}{\tau_{fast}}\right) + A_{slow}(q)\exp\left(\frac{-t}{\tau_{slow}}\right) \tag{12}$$

$E_{fast}(q,t)$ and $E_{slow}(q,t)$ are respectively the fast and the slow electric scattered field and are fluctuating independently. τ_{fast} and τ_{slow} are respectively the fast and the slow relaxation time. $A_{fast}(q)$ and $A_{slow}(q)$ are the corresponding amplitudes. As shown later on, the systems for which a single relaxation process is observed correspond to the dilute regime, whereas the other systems characterized by a double relaxation are overlapped solutions. Similar results are observed for the three investigated ionic strengths.

In the overlapped regime, characterized by two distinct relaxation processes, we proceed as follows: first we plot in semilog coordinates the function $g^{(1)}(q,t)$ obtained by means of eq 9. An example is given in Figure 2 relative to a 0.3 M CH_3COOH + 0.05 M CH_3COONa solution of chitosan at $c = 2 \times 10^{-3}$ g/cm³. The scattering angle θ is equal to 90°. One clearly sees in the long time scale an asymptotic behavior that can be described to the first approximation by a straight line. From the slope and the intercept of the straight line we can determine the slow relaxation time τ_{slow} and the corresponding relative amplitude A_{slow}. The first cumulant associated with the fast mode τ_{fast} can be obtained from the initial slope of $g^{(1)}(q,t)$. In the case of the dilute solution at $c = 3 \times 10^{-4}$ g/cm³, we only see one relaxation.

Another method to determine τ_{slow} and τ_{fast} is the Contin method based on the inverse Laplace transform of $g^{(1)}(q,t)$.[26] If the spectral profile of the scattered light can be described by a multi-Lorentzian curve, then $g^{(1)}(q,t)$ can be written as

$$g^{(1)}(q,t) = \int_0^\infty G(\Gamma)\exp(-\Gamma t)\,d\Gamma \tag{13}$$

where $G(\Gamma)$ is the normalized decay constant distribution. This method is more appropriate for solutions characterized by several relaxations mechanisms (e.g., a mixture of polymers and aggregates or solutions characterized by two relaxation times). For commodity, we were also using the Contin method.[26] Figure 3 shows a typical example of results obtained by applying the Contin method to our data for a dilute and an overlapped solution. We clearly distinguish slow and fast modes well separated in time for overlapped solutions. It is found to a quite good accuracy that the relaxation times obtained from Contin method coincides with the relaxation times obtained from the method described earlier (Figure 2).

3. Results and Discussion

3.1. Static Light Scattering in Dilute Regime. A classical graphical technique for simultaneously extrapolating light-scattering data in the dilute regime to both zero angle and zero concentration is the Zimm plot. This is achieved by plotting $Kc/I(q,c)$ as a function of $q^2 + 10c$ as shown in Figure 4 where K is the scattering constant (see eq 5) and the factor 10 a chosen constant
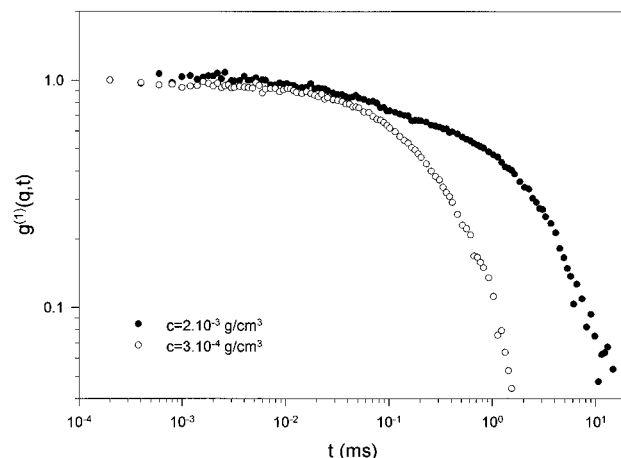

Figure 1. A log–log representation of $g^{(1)}(q,t)$ for $\theta = 90°$ relative to 0.3 M CH_3COOH + 0.05 M CH_3COONa solutions of chitosan at $T = 25$ °C and at polymer concentrations $c = 3 \times 10^{-4}$ g/cm³ (○) and $c = 2 \times 10^{-3}$ g/cm³ (●).
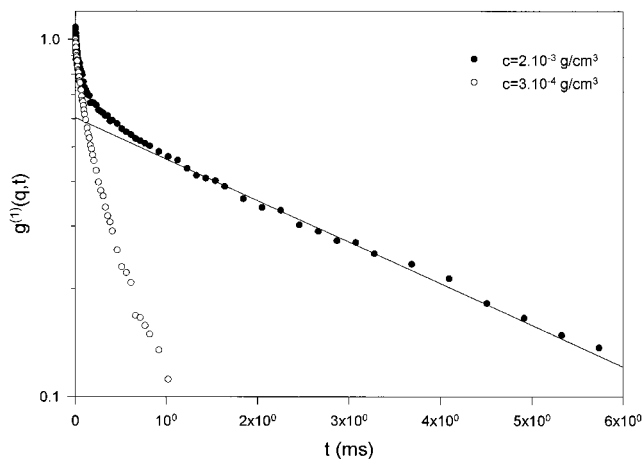

Figure 2. Semilog representation of $g^{(1)}(q,t)$ for $\theta = 90°$ relative to 0.3 M CH_3COOH + 0.05 M CH_3COONa solutions of chitosan at $T = 25$ °C and at polymer concentrations $c = 3 \times 10^{-4}$ g/cm³ (○) and $c = 2 \times 10^{-3}$ g/cm³ (●). The straight line represents the fit in the long time scale for the more concentrated solution at $c = 2 \times 10^{-3}$ g/cm³.

to give a convenient spacing of the data points on the graph. The concentrations used for the Zimm plot are in dilute regime and are respectively equal to $c = 10^{-4}$, 2×10^{-4}, 3×10^{-4}, and 4×10^{-4} g/cm³. The solvent is a 0.3 M CH_3COOH + 0.05 M CH_3COONa solution, and the temperature is equal to 25 °C. The data points on the grid corresponding to a given angle are then extrapolated to zero concentration, and similarly the points at a given concentration are extrapolated to zero angle. The inverse of the weight-average molecular weight, M_w, is obtained from the intercept of the $q^2 = 0$ curve, according to eq 14, and the second virial coefficient, A_2, is obtained from the slope ($2A_2 = $ slope).

$$\left(\frac{Kc}{I}\right)_{q^2=0} = \frac{1}{M_w} + 2A_2 c \tag{14}$$

The intercept of the $c = 0$ curve again gives the inverse of the molecular weight, and the initial slope is proportional to the radius of gyration as described by the following equation:
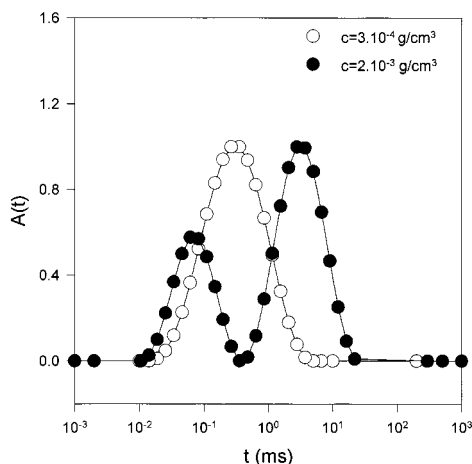
Figure 3. Normalized distribution function of decay times $A(t)$ for $\theta = 90°$ obtained using the Contin method for 0.3 M CH_3COOH + 0.05 M CH_3COONa solutions of chitosan at polymer concentrations $c = 3 \times 10^{-4}$ g/cm^3 (○) and $c = 2 \times 10^{-3}$ g/cm^3 (●).
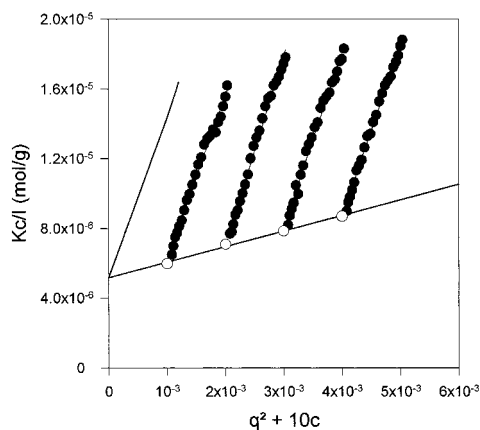

Figure 4. Zimm plot of the polyelectrolyte chitosan at $T = 25$ °C. The solvent is a 0.3 M CH_3COOH + 0.05 M CH_3COONa solution. Points (○) are extrapolations to zero wave vector, and solid lines represent best fits.

$$\left(\frac{Kc}{I}\right)_{c=0} = \frac{1}{M_w}\left[1 + \frac{q^2 R_G^2}{3}\right] \tag{15}$$

For the average weight molecular weight and the radius of gyration, we find $M_w = (194000 \pm 5000)$ and $R_G = (70 \pm 10)$ nm, respectively. The determined value of the molecular weight is in very good agreement with the commercial one. The value of the radius of gyration is pretty high, characteristic of semirigid polymer. The ratio of the hydrodynamic radius ($R_H = 48$ nm) and the radius of gyration is equal to 0.68 (see paragraph 3.3 and Table 1 for the determination of the hydrodynamic radius). Actually this ratio is equal to 0.8 for flexible monodisperse Gaussian chains[27] in a Θ solvent. Note that the polydispersity of our polymer is equal to 1.3 and that we are in a good solvent. For polydisperse, flexible chain in a good solvent this ratio can be as low as 0.54.[28] The positive sign of the second virial coefficient, $A_2 = (4.47 \pm 0.50) \times 10^{-3}$ cm$^3 \cdot$g$^{-2} \cdot$mol, indicates that at these conditions the 0.3 M CH_3COOH/ 0.05 M CH_3COONa medium is a good solvent for chitosan. Actually the value of the second virial coefficient is increasing with the decrease of the excess salt concentration (see Table 1).[1] A similar trend in the dependence of the second virial coefficient of polyelectrolytes on the

salt concentration was observed in previous scattering experiments.[29] The increase of the second virial coefficient is characteristic of the increase of the expansion of the polyelectrolyte chain and electrostatic repulsion interaction. We will see in part 3.3 that the behavior of the second dynamical virial coefficient k_D with the excess salt concentration is similar. Values of R_G and A_2 for the three studied salt concentrations are collected in Table 1.

The static light-scattering data obtained for more concentrate solutions are shown in the next part.

3.2. Combined Static and Dynamic Light Scattering. Another interesting discussion can be made by examination of the behavior of the relative amplitudes A_{slow} and A_{fast}. The sum of the amplitudes of the two modes is equal to 1.

$$A_{fast}(q) + A_{slow}(q) = 1 \tag{16}$$

It is worth noting that in fact these amplitudes are dependent on the scattering wave vector **q**, as shown in Figure 5. Figure 5a shows the q dependence of the ratio A_{slow}/A_{fast} for a 0.3 M CH_3COOH + 0.05 M CH_3COONa solution of chitosan at a concentration $c = 2 \times 10^{-3}$ g/cm^3 and at a temperature $T = 25$ °C. The variation of A_{slow}/A_{fast} extrapolated at zero-wave vector with the polymer concentration can be observed in Figure 5b. A similar behavior is observed for the two other salt concentrations. At fixed polymer concentration, no variations of the slow relative amplitude with the investigated salt concentrations were distinguished.

These amplitudes of the two modes measured by dynamic light scattering can be used to analyze the static light-scattering results.[30] Defining $I_{fast}(q)$ and $I_{slow}(q)$ as the time average intensities associated with the fluctuations of polymer concentration with respectively short and long relaxation times and using the normalization condition

$$g^{(1)}(q,0) = A_{fast}(q) + A_{slow}(q) \tag{17}$$

we obtain

$$I_{fast}(q) = A_{fast}(q)I(q)$$
$$I_{slow}(q) = A_{slow}(q)I(q) \tag{18}$$

with

$$I_{fast}(q) + I_{slow}(q) = I(q) = I_{total}(q) \tag{19}$$

The dependence on polymer concentration of the total scattered intensity $I_{total}(q = 0)$, of the scattered intensity associated with the fast decay mode $I_{fast}(q = 0)$ and of the scattered intensity associated with the slow decay mode $I_{slow}(q = 0)$, is shown in Figure 6. The intensities are extrapolated to zero wave vector, the solvent is a 0.3 M CH_3COOH + 0.05 M CH_3COONa solution, and the temperature is still equal to 25 °C. $I_{fast}(q = 0)$ and $I_{slow}(q = 0)$ are only plotted for polymer concentrations larger than the concentration c^*, where slow and fast modes are observed. As shown later on, the systems for which a single relaxation process is observed correspond to the dilute regime, whereas the other systems characterized by a double relaxation are overlapped solutions. It is worth noting that the total and the slow intensities are increasing with polymer concentration even after the overlap concentration c^* is reached. For

Table 1. Variation of the Dynamic Second Virial Coefficient, of the Diffusion Coefficient at Infinite Dilution, of the Hydrodynamic Radius, of the Radius of Gyration, of the Second Virial Coefficient, of the Overlap Concentration c^* Deduced from Figure 8, and of the Intrinsic Viscosity as a Function of the Excess of Salt Concentration (Sodium Acetate) for 0.3 M Acetic Acid Solutions of Chitosan at Temperature $T = 25$ °C

[CH$_3$COONa] (M)	k_D (cm^3/g)	$10^{-6}D_0$ (nm^2/s)	R_H (nm)	R_G (nm)	$10^3 A_2$ (cm^3·g^{-2}·mol)	c^* (g/cm^3)[a]	$[\eta]$ (cm^3/g)
0.05	588 ± 60	5.1 ± 0.5	48 ± 4	70 ± 10	4.47 ± 0.50	(5.5 ± 0.5) × 10^{-4}	1200 ± 100
0.1	300 ± 30	6.5 ± 0.5	38 ± 4	54 ± 8	2.70 ± 0.20	(6.5 ± 0.5) × 10^{-4}	1100 ± 100
0.2	37 ± 5	8.6 ± 0.5	29 ± 4	42 ± 6	1.10 ± 0.10	(1 ± 0.05) × 10^{-3}	900 ± 100

[a] Deduced from Figure 8.

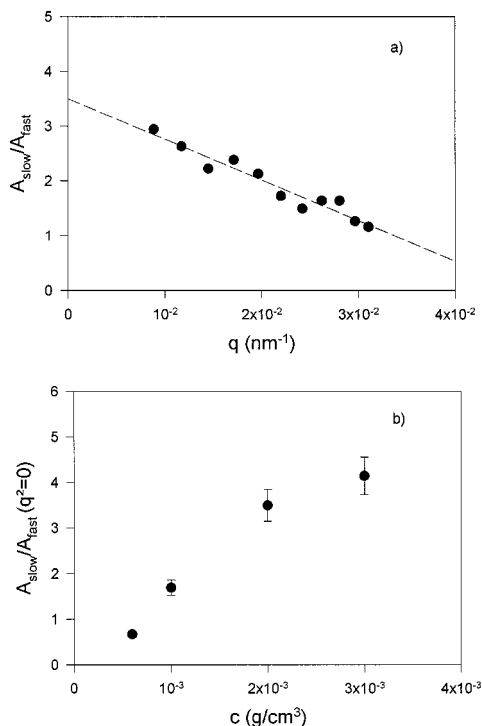**Figure 5.** Scattering wave vector dependence (a) of A_{slow}/A_{fast} for a $c = 2 \times 10^{-3}$ g/cm^3 solution and polymer concentration dependence (b) of A_{slow}/A_{fast} ($q^2 = 0$). The solvent is a 0.3 M CH$_3$COOH + 0.05 M CH$_3$COONa solution at temperature $T = 25$ °C. The dashed line in plot a represents the fit of the data.

the variation of the fast intensity with polymer concentration, we observe a slight decrease. We will see in the next part that the variations of $I_{total}(q = 0)$ in dilute regime and of $I_{fast}(q = 0)$ with polymer concentration are typical for neutral polymer solutions in the dilute and in the semidilute regime, the transition between these two regimes occurring at the concentration c^*.

3.3. Single Relaxation Mode and Fast Relaxation Mode. The inspection of Figure 7, representing the variation of the product $\tau_{fast}q^2$ with q for different polymer solutions shows clearly that the fast mode is a diffusive one with characteristic time τ_{fast} inversely proportioned to q^2. In the dilute regime only one cooperative mode is observed. Thus, it is possible to calculate for each polymer concentration a diffusion coefficient D using eq 11.

Figure 8 shows the polymer concentration dependence of D for 0.3 M CH$_3$COOH + CH$_3$COONa solutions of chitosan at $T = 25$ °C. Three excess of salt concentrations (three ionic strengths) were investigated: 0.05, 0.1, and 0.2 M. The diffusion coefficient increases slowly with c at first, then more rapidly as c$[\eta]$ exceeds about unity (and where the two modes appear), where $[\eta]$ is the intrinsic viscosity of the solution and η the solution
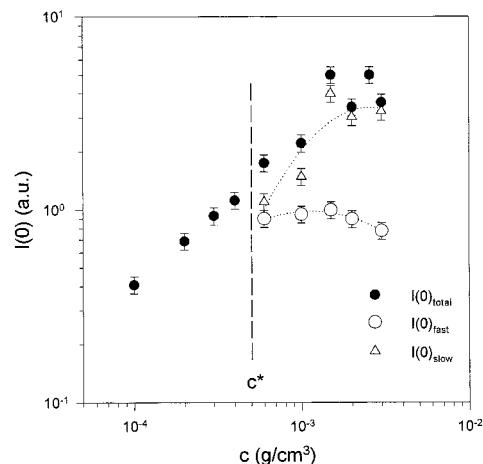

Figure 6. Dependence of the total scattering intensity (●), of the scattering intensity associated with the fast mode (○) and of the scattering intensity associated with the slow mode (△) on the polymer concentration. The intensities are extrapolated to zero-wave vector and the solvent is a 0.3 M CH$_3$COOH + 0.05 M CH$_3$COONa solution at temperature $T = 25$ °C. The vertical dashed line represents the transition between dilute and overlapped regime.
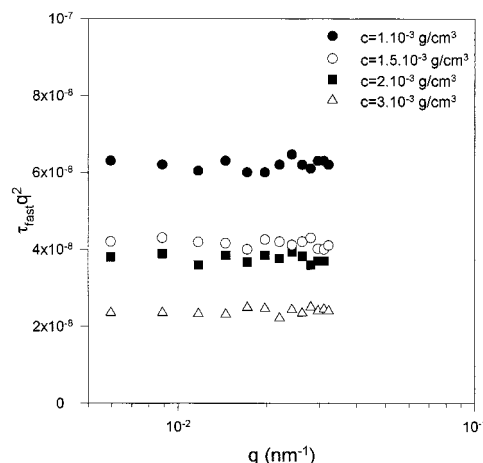

Figure 7. Variation of $\tau_{fast}q^2$ with q measured in 0.3 M CH$_3$COOH + 0.05 M CH$_3$COONa solutions with the following polymer concentrations: $c = 1 \times 10^{-3}$ g/cm^3 (●), $c = 1.5 \times 10^{-3}$ g/cm^3 (○), $c = 2 \times 10^{-3}$ g/cm^3 (■), and $c = 3 \times 10^{-3}$ g/cm^3 (△).

viscosity

$$[\eta] = \frac{\eta - \eta_s}{\eta_s c} \quad c \to 0 \tag{20}$$

Values of $[\eta]$ for the different studied excesses of salt concentration are collected in Table 1.

In dilute polyelectrolyte solution regime, characterized by a single diffusive relaxation, it is observed that the apparent diffusion coefficient D measured is a linear function of the polyelectrolyte concentration
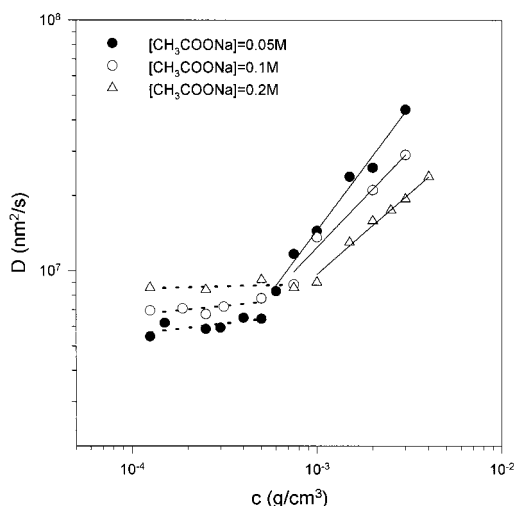
Figure 8. Dependence of the diffusion coefficient on the polymer concentration for three excesses of salt concentrations: 0.05 M (●), 0.1 M (○), and 0.2 M (△). Black lines represent fits of the data in the overlapped regime and dashed lines represent linear least squares best fits in the dilute virial regime. In the overlapped regime (when D is strongly increasing with c) D values are obtained from the fast relaxation time. The experimental error is equal to 10%.

$$D = D_0(1 + k_D c + ...) \quad (21)$$

with D the apparent diffusion coefficient, D_0 the apparent diffusion coefficient at infinite dilution, k_D the diffusion second virial coefficient, and c the polyelectrolyte concentration. The separation between the dilute virial regime and the overlapped regime is characterized by the critical overlap concentration c^*, i.e., when $c[\eta]$ is about unity.[31] The polyelectrolyte concentration dependence of the apparent diffusion coefficient is linear for all conditions employed (three ionic strengths) and shows that the virial expansion can be limited to the second virial coefficient in the dilute concentration range. The positive sign of the k_D indicates that the medium is a good solvent for chitosan. Figure 8 shows that on decreasing the ionic strength (salt concentration) the polyelectrolyte concentration dependence of the apparent diffusion coefficient becomes stronger. The obtained values for D_0 and k_D with linear least-squares best fits are collected in Table 1. With decreasing ionic strength (salt concentration), D_0 becomes smaller due to expansion of the polyelectrolyte coil. Using the Stokes–Einstein equation (see eq 11), we can calculate the hydrodynamic radius R_H using the value of D_0. Values of R_H for the three studied ionic strengths are also reported in Table 1. The dependence of k_D on salt concentration is predicted by the small ion–polyion coupled mode theory, as reviewed by Schurr and Schmitz.[32] The molecular theory of Imai and Mandel[33] also predicts this. These authors showed that k_D is proportional to the inverse of the salt excess concentration. This k_D dependence with salt concentration was experimentally found by Smits et al.[34] and by Tanahatoe et al.[29] for linear highly charge polyelectrolyte and is also in good agreement with our data.

The overlap concentration can be estimated from Figure 8 (values of c^* are collected in Table 1). This concentration corresponds to the transition between the two regimes observed in the curves characterizing the variation of the diffusion coefficient with polymer concentration. After the overlap concentration c^* (solutions are characterized by two relaxations), the fast

diffusion coefficient derived from the fast relaxation increases consequently with polymer concentration as shown in Figure 8. In this regime, the variation of the fast diffusion coefficient with polymer concentration can be described by a power law depending on the ionic strength: $D \approx c^{0.99}$, $D \approx c^{0.78}$, and $D \approx c^{0.65}$ for sodium acetate concentration (CH_3COONa) equal to 0.05, 0.1, and 0.2 M, respectively. The experimental error on the exponent values is equal to 10%. Moreover, the intensity associated with the fast mode extrapolated to zero wave vector $I_{fast}(q = 0)$ is decreasing with polymer concentration in the overlapped regime. Since the decrease is small, it is difficult to fit the data and obtain a power law describing the variation of $I_{fast}(q = 0)$ with c (see Figure 6).

de Gennes developed a scaling theory for semidilute solutions in thermodynamically good solvents.[31] The main prediction of this theory is that the dynamical behavior of the solution can be described in terms of a single characteristic length, that is, the correlation length ξ. Then the cooperative diffusion coefficient D is given by

$$D = \frac{kT}{6\pi\eta_s\xi_H} \quad (22)$$

where ξ_H is the hydrodynamic correlation length that scales like the static correlation length ξ and η_s is the solvent viscosity. The correlation length ξ and consequently the cooperative diffusion coefficient D follow simple scaling laws to dilution according to[31]

$$\xi \approx c^{-0.77} \quad \text{and} \quad D \approx c^{0.77} \quad (23)$$

Further information on the concentration dependence of the correlation length is given by the zero-q limit of the scattered intensity. In the semidilute regime, the scattered intensity becomes independent of the molecular weight and its contribution dependence can be described by a power law of the form[31]

$$I(0) \approx c^{-0.31} \quad (24)$$

still assuming good solvent conditions.

In the overlapped regime, our results show that the variations of D and $I_{fast}(q = 0)$ with polymer concentration for 0.1 and 0.2 M added salt solutions are consistent with the behavior expected for a semidilute solution in good solvent. In this regime the fast diffusion coefficient follows a power law, with a power law that depends on the ionic strength. In the 0.05 M added salt CH_3COONa solution, the diffusion coefficient can be characterized by an exponent equal to 0.99, larger than the theoretical value for neutral polymer. For this salt concentration, all the charges may not be screened even if this salt concentration is not small and close to 0.1 and 0.2 M. To our knowledge, there is no theoretical model predicting the variation of the diffusion coefficient with polymer concentration for not screened or not totally screened polyelectrolyte solutions. The fast mode should correspond to the contribution of an overlapped solution, and the associated fluctuations of concentration relax by a cooperative diffusion mechanism of the meshes of the network. Using the Stokes–Einstein equation (see eq 22), the calculated mesh size of the network (ξ_H) ranges between 30 and 7 nm in the investigated concentration range (see Figure 10). So experiments were done in the regime where the mesh size is larger
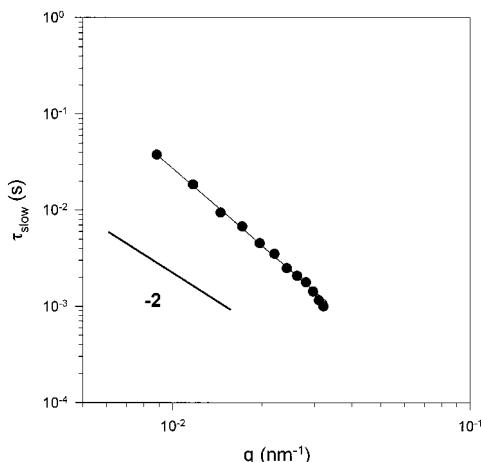
Figure 9. Variation of the slow characteristic time with q measured in 0.3 M CH$_3$COOH + 0.05 M CH$_3$COONa solution with polymer concentration $c = 2 \times 10^{-3}$ g/cm^3.
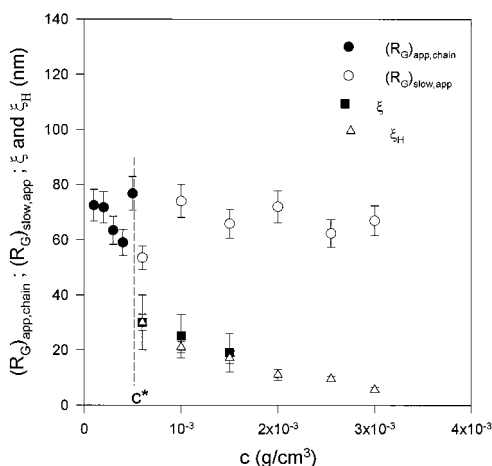

Figure 10. Variation of the apparent radius of gyration of the chains in dilute regime $(R_G)_{app,chain}$ (●), of the associations in overlapped regime $(R_G)_{slow,app}$ (○), of the correlation length ξ (■), and of the hydrodynamic correlation length ξ_H (△) with polymer concentration for 0.3 M CH$_3$COOH + 0.05 M CH$_3$-COONa solutions at temperature $T = 25$ °C. The dashed line represents the transition between dilute and overlapped regime.

than the persistence length for almost the whole investigated concentration range. Values of ξ_H as a function of the polymer concentration are plotted in Figure 10. One can estimate the static correlation length ξ from $I_{fast}(q,c)$ for each polymer concentration in the semidilute regime.

$$I_{fast}(q,c) = I_{fast}(0,c)(1 - q^2\xi^2) \qquad (25)$$

For the 0.3 M CH$_3$COOH + 0.05 M CH$_3$COONa system, the value of the correlation length was determined for polymer concentration equal to 6×10^{-4}, 10^{-3}, and 1.5×10^{-3} g/cm^3. For larger concentrations, the size associated with the fast mode is too small to exhibit a q dependence of $I_{fast}(q,c)$ in the q range investigated by light scattering. Values of ξ are also plotted in Figure 10. These values are in very good agreement with the ξ_H values determined from dynamic light-scattering measurements.

3.4. Origin of the Slow Mode. The slow relaxation mode appears only for polymer concentrations larger than the overlap concentration c^*. Slow relaxation times are characterized by a stronger q dependence (Figure

9) than that found for the fast relaxation mode. This dependence can be described by a power law behavior with exponents ranging between -2 and -2.8 depending on the polymer concentration. These results are observed for the three studied salt concentrations. At fixed polymer concentration, no variations of the relative slow amplitude with ionic strength were observed. Note that the three salt concentrations are very close. Figure 9 shows the variation of the slow relaxation time with q for a 0.3 M CH$_3$COOH + 0.05 M CH$_3$COONa solution of chitosan at a polymer concentration $c = 2 \times 10^{-3}$ g/cm^3 and at the temperature $T = 25$ °C. In this example the dependence of the slow relaxation time with q is described by a power law characterized by an exponent equal to -2.5. Variations of τ_{slow} with q for the other concentrations are not plotted in Figure 9 for clarity. When the polymer concentration is increased, the slow relaxation time is also increased.

The presence of a slow mode is not an uncommon feature and has been observed in many different systems including low ionic strength polyelectrolyte solutions,[20] high ionic strength polyelectrolyte solutions,[22,23] associating polymer solutions,[30] linear neutral polymer systems in good[35] and Θ solvents[36] and nearly all classes of charged macromolecular systems in dilute and in concentrate solutions. Although the generic name of slow mode is widely used, its physical origin may differ according to the system considered. In particular, dynamic coupling of elementary processes, coupling of stress and polymer concentration fluctuations,[35] or diffusion of large particle aggregates[22,23] or of polymer domains[20] are possible mechanisms that might be responsible for a slow component in the time autocorrelation function of the scattered electric field. However, in the present study the slow mode appears only for polymer concentrations larger than the overlap concentration c^*, the dilute solutions showing a classical good solvent behavior (see part 3.3). Moreover, our experiments were carried out under high ionic strength polyelectrolyte solutions (0.05, 0.1, and 0.2 M excesses of salt concentration solutions) where long-range electrostatic interactions are certainly screened. The variations of the relative slow amplitude (Figure 5a), variations of the slow relaxation time (Figure 9) as a function of scattering wave-vector, and variations of the slow amplitude (Figure 5b) and of the associated scattering intensity (Figure 6) with the polymer concentration should help us to decide which mechanism is suitable for a given system.

In the present case we have showed that the slow amplitude, A_{slow}, and the slow relaxation time, τ_{slow}, are q-dependent. In fact, in the semidilute regime, the network is deformed when fluctuations of polymer concentration are relaxing cooperatively.[35,37-40] This network deformation is responsible for a local stress fluctuation relaxing on a much longer time scale. The amplitude of this viscoelastic relaxation is directly related to the ratio of the elastic and osmotic modulus.[37] However, an experimental study of Buhler et al.[35] and detailed derivations of this model[38-40] show no q dependence for the slow viscoelastic relaxation time and for the associated slow relative amplitude, contrary to our results. Moreover, the increase of A_{slow} with the decrease of q, the increase of $I_{slow}(q = 0)$ and of $A_{slow}(q = 0)$ with polymer concentration suggest that the slow mode is due to the formation of aggregates, associations or domains. An alternative, in which the slow mode

arises from long-range electrostatic interactions, would also undergo dramatic reduction in the intensity, not observed in this study. Such results are consistent with the model where the slow relaxation is considered to be due to aggregates, to large objects or to multichain domains that are diffusing in the solution. In the case of multichain domains, we can describe the q dependence of the slow relaxation time as

$$t_{slow}^{-1}(q) = D'q^2(1 + Aq^2 R'^2_{G,app}) \quad qR'_{G,app} < 1 \quad (26)$$

where D' is a diffusion coefficient, $R'_{G,app}$ an apparent radius of gyration of the domains, and A a constant depending on the structure and the polydispersity of the domains. This approach was used to analyze experiments realized on polyelectrolyte solutions.[16] Equation 26 could explain the q dependence of τ_{slow} in our experiments, i.e., $\tau_{slow} \sim q^{-x}$, with x ranging between 2 and 2.8 depending on the polymer concentration. Presence of associations seems very likely in solutions where associations through hydrophobic interactions are possible.[41] So we have checked the effect of the degree of N-acetylation of chitosan, and no changes in the autocorration function were observed. So the degree of N-acetylation is not related to any polymer associations or multichain domains.

The results of Tanahatoe et al.[22,23] are closer to our results. The authors have studied semidilute solutions of the flexible highly charged polyelectrolyte sodium polystyrenesulfonate with dynamic light scattering over a wide polyelectrolyte concentration range. Double exponential correlation functions were also measured. The apparent fast and slow diffusion coefficients were determined for three ionic strengths. The slow diffusion coefficient depends on the polymer concentration and on the ionic strength over the whole studied concentration range. The slow mode was interpreted as caused by aggregates or domains that form in semidilute and concentrate solutions. The dimensions of these aggregates decrease with decreasing polyelectrolyte concentration and with increasing ionic strength.[23,42] In the aggregates or large domains approach, the scattering intensity associated with the slow mode $I_{slow}(q,c)$ can be analyzed as

$$\frac{Kc_{slow}}{I_{slow}(q,c_{slow})} = \frac{1}{M_{w,slow}}\left(1 + q^2\frac{R_{G,slow}^2}{3}\right) + 2A_2 c_{slow} \quad (27)$$

where c_{slow} is the concentration related to the slow mode (the aggregates concentration). The sum of c_{slow} and c_{fast} (the concentration associated with the fast mode) is equal to the total polymer concentration c

$$c_{slow} + c_{fast} = c \quad (28)$$

$R_{G,slow}$ is the radius of gyration of the aggregates or associations. In the aggregates or some state of associations model, the slow mode scattering may well arise from a small fraction of higher molecular weight components, of unknown concentration c_{slow} and mass $M_{w,slow}$. Figure 10 shows the variation of the apparent radius of gyration of the aggregates with polymer concentration for 0.3 M CH_3COOH + 0.05 M CH_3-COONa solutions at $T = 25$ °C. In Figure 10 are also plotted the correlation length in semidilute regime and the apparent radius of gyration of the polymer chain in the dilute regime. The apparent radius of gyration of

the single chain in dilute regime is slightly decreasing with polymer concentration as expected for dilute solutions in good solvent with $R_{G,chain}$ invariant with c. The apparent radius of gyration of the aggregates $(R_G)_{slow,app}$ was determined using the following relation

$$I_{slow}(q,c_{slow}) = I_{slow}(0,c_{slow})[1 - {}^1/_3 q^2(R_G^2)_{slow,app}]$$
$$q(R_G)_{slow,app} \ll 1 \quad (29)$$

where $I_{slow}(0,c_{slow})$ is the slow scattering intensity at zero angle and $(R_G)_{slow,app}$ is an apparent radius of gyration for the domains or the aggregates. Data reveal $(R_G)_{slow,app}$ values of 70 ± 10 nm over the whole overlapped regime. The concentration dependence of $(R_G)_{slow,app}$ requires care. Actually the real radius of gyration of the associations or aggregates $R_{G,slow}$ is larger than the apparent one

$$(R_G^2)_{slow,app} = \frac{3\partial\left[\dfrac{I_{slow}(0,c_{slow})}{I_{slow}(q,c_{slow})}\right]}{\partial q^2} = \frac{(R_G^2)_{slow}}{1 + 2A_2 M_{w,slow} c_{slow}} \quad (30)$$

$(R_G^2)_{slow,app}$ might approximate $(R_G^2)_{slow}$ only if $2A_2$-$M_{w,slow}c_{slow} \ll 1$. Actually we cannot ignore the effect of the huge virial coefficient A_2 determined in part 3.1. So even if the aggregates are considered to be dilute, i.e., $c_{slow} \ll c$, the factor $2A_2 M_{w,slow}c_{slow}$ cannot be neglected, and then the real radius of gyration of the associations must be larger than 70 nm and is increasing with polymer concentration.

First of all, note that no differences between the 0.1 and 0.2 μm filtration measurements were made. The slow mode is not eliminated and is almost not altered quantitatively in character by different filtrations and does regain a definite well-characterized state. This is the reason we think the slow mode is related to physical associations or domains in semidilute solutions. In the present work the slow relaxation time presents an approximately q^2 dependence (see Figure 9), characteristic of a cooperative diffusion mechanism. In analogy with dilute polymer solutions, we would write

$$\tau_{slow}^{-1} = \frac{kT\,q^2}{6\pi\eta R_H} \quad (31)$$

where η is viscosity. For dilute polymer solution, η would be the viscosity of the solvent and R_H the hydrodynamic radius of the polymer. Now we can argue that if we are in the presence of large objects immersed in an overlapped solution, the viscosity η of eq 31 should be much larger than the solvent viscosity and should tend to equal the macroscopic viscosity and R_H should represent the hydrodynamic radius of the polymer associations. One can use eq 31 and the solution viscosity to estimate the size of these associations. The variation of the estimated apparent hydrodynamic radius of the associations as a function of the polymer concentration is represented in Figure 11 for the three different ionic strengths studied. The dimensions of these associations decrease with decreasing polymer concentration and with decreasing ionic strength (a decrease of the ionic strength is characteristic of a decrease of the attractive van der Waals interactions). A slow mode corresponding to associations or aggregates is essentially not observed with solutions in good
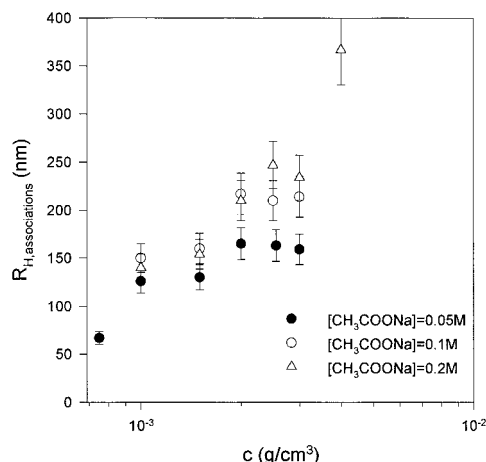
Figure 11. Variation of the hydrodynamic radius of the associations in the overlapped regime obtained with eq 31 with polymer concentration for 0.3 M CH₃COOH + CH₃COONa solutions. The concentration of excess of salt is equal to 0.05 M (●), 0.1 M (○), and 0.2 M (△).

solvents, but rather requires a solution under Θ conditions with $A_2 \approx 0$ to be a dominant effect. A slow mode is also usually observed in low ionic strength solution. So we think the high rigidity of chitosan could be related to some state of physical polymer associations in semidilute regime.

4. Conclusion

We have presented the results of the light-scattering study of semiflexible polyelectrolyte chitosan in high ionic strength solutions.

In the dilute regime, typical good solvent behavior is found (Figure 4). However, in the semidilute regime, the time autocorrelation function of the scattered electric field measured by dynamic light scattering is found to be bimodal (Figure 1). To understand the origin of the fast and the slow mode, the scattering wave vector dependencies for the scattering intensity and for the amplitudes and characteristic times associated with the relaxation modes were carefully analyzed. Combination of the static and dynamic techniques provides a powerful tool to better understand the physical mechanisms that are at the origin of dynamical behavior of this semirigid system (Figure 6). The short time relaxation has a typical q^2 dependence (Figure 7), characteristic of diffusion and the long time relaxation an approximately q^2 dependence (Figure 9). The fast mode is attributed to the relaxation of polymer concentration fluctuations characterized by a cooperative diffusion mechanism of the polymer network meshes, i.e., the correlation mesh.

The slow mode is attributed to the formation of physical polymer associations in the semidilute regime. We think the high rigidity of this polymer is related to the origin of some state of associations. The dimensions of these associations increase with increasing polymer concentration. The apparition of associations is usually not observed with solutions in good solvent characterized by a high ionic strength, but rather requires a solution under Θ conditions or a solution under low ionic strength conditions.

In this respect, combined static and dynamic light-scattering techniques appear to be very powerful to analyze the structural and dynamical behavior of semirigid polymer systems. X-ray experiments are scheduled

to study the structure of these associations. Also new experiments concerning the variation of the molecular weight and of the persistence length in high and low ionic strength solutions will be presented in a forthcoming paper.

References and Notes

(1) Rinaudo, M.; Pavlov, G.; Desbrière, J. *Polymer* **1999**, *40*, 7029.
(2) Odijk, T. *J. Polym. Sci., Polym. Phys.* **1977**, *15*, 477.
(3) Skolnick, J.; Fixman, M. *Macromolecules* **1977**, *10*, 944.
(4) Fixman, M. *J. Chem. Phys.* **1982**, *76*, 6346.
(5) Le Bret, M. *J. Chem. Phys.* **1982**, *76*, 6243.
(6) Manning, G. S. *J. Chem. Phys.* **1969**, *51*, 924.
(7) Lin, S. C.; Lee, W. I.; Schurr, J. M. *Biopolymers* **1978**, *17*, 1041.
(8) Mathiez, P.; Mouttet, C.; Weisbuch, G. *Biopolymers* **1981**, *20*, 2381.
(9) Schmitz, K. S.; Lu, M.; Gauntt, J. *J. Chem. Phys.* **1983**, *78*, 5059.
(10) Drifford, M.; Dalbiez, J. P. *Biopolymers* **1985**, *24*, 1501.
(11) Koene, R. S.; Mandel, M. *Macromolecules* **1983**, *16*, 973.
(12) Sedlák, M.; Konák, C.; Stepánek, P.; Jakes, J. *Polymer* **1987**, *28*, 873.
(13) Schmitz, K. S.; Yu, J. *Macromolecules* **1988**, *21*, 484.
(14) Schmidt, M. *Makromol. Chem., Rapid Commun.* **1989**, *10*, 89.
(15) Förster, S.; Schmidt, M.; Antonietti, M. *Polymer* **1990**, *31*, 781.
(16) Sedlák, M.; Amis, E. J. *J. Chem. Phys.* **1992**, *96*, 817.
(17) Ermi, B. D.; Amis, E. J. *Macromolecules* **1996**, *29*, 2703.
(18) Topp, A.; Belkoura, L.; Woermann, D. *Macromolecules* **1996**, *29*, 5392.
(19) Nerling, W.; Nordmeir, E. *Polym. J.* **1997**, *29*, 795.
(20) Ermi, B. D.; Amis, E. J. *Macromolecules* **1998**, *31*, 7378.
(21) Reed, W. F. *Macromolecules* **1994**, *27*, 873.
(22) Tanahatoe, J. J.; Kuil, M. E. *J. Phys. Chem. B* **1997**, *101*, 9233.
(23) Tanahatoe, J. J.; Kuil, M. E. *J. Phys. Chem. B* **1997**, *101*, 10839.
(24) Cummins, H. Z.; Pike, E. R. *Photon Correlation and Light Beating Spectroscopy*; Plenum Press: New York, 1974.
(25) Koppel, D. E. *J. Chem. Phys.* **1972**, *57*, 4814.
(26) Provencher, S. W. *Makromol. Chem.* **1985**, *82*, 632.
(27) Schmidt, M.; Burchard, W. *Macromolecules* **1981**, *14*, 210.
(28) Akcasu, A. Z.; Benmouna, M.; Alkhafaji, S. *Macromolecules* **1981**, *14*, 147.
(29) Tanahatoe, J. J.; Kuil, M. E. *Macromolecules* **1997**, *30*, 6102.
(30) Klucker, R.; Munch, J. P.; Schosseler, F. *Macromolecules* **1997**, *30*, 3839.
(31) De Gennes, P. G. *Scaling Concepts in Polymer Physics*; Cornell University Press: Ithaca, NY, 1979.
(32) Schurr, J. M.; Schmitz, K. S. *Annu. Rev. Phys. Chem.* **1986**, *37*, 271.
(33) Imai, N.; Mandel, M. *Macromolecules* **1982**, *15*, 1562.
(34) Smits, R. G.; Kuil, M. E.; Mandel, M. *Macromolecules* **1993**, *26*, 6808.
(35) Buhler, E.; Munch, J. P.; Candau, S. J. *J. Phys. II Fr.* **1995**, *5*, 765.
(36) Adam, M.; Delsanti, M. *Macromolecules* **1985**, *18*, 1760.
(37) Brochard, F.; de Gennes, P. G. *Macromolecules* **1985**, *10*, 121.
(38) Semenov, A. N. *Physica A* **1990**, *166*, 263.
(39) Doi, M.; Onuki, A. *J. Phys. II Fr.* **1992**, *2*, 1631.
(40) Wang, C. H. *Macromolecules* **1992**, *25*, 1524.
(41) Aiba, S. *Int. J. Biol. Macromol.* **1991**, *13*, 40.
(42) Ray, J.; Manning, G. S. *Langmuir* **1994**, *10*, 2450.

MA991309+